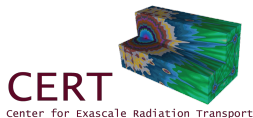


# A High-Order Low-Order Algorithm with Exponentially-Convergent Monte Carlo for Thermal Radiative Transfer

Simon Bolding, Matt Cleveland, and Jim Morel

4 August 2016



We are interested in modeling thermal radiation transport in the high energy density physics regime

Modeling materials under extreme conditions

Temperatures  $\mathcal{O}(10^6)$  K or more

Photon radiation transports through a material

Significant **energy** may be exchanged

We want to improve efficiency of Monte Carlo calculations

e.g., inertial confinement fusion, supernovae, et. al.

Our method has been applied to a simplified model:  
the 1D frequency-integrated radiative transfer equations

Energy balance equations for radiation and material.

Radiation intensity  $I(x, \mu, t)$ , material temperature  $T(x, t)$

$$\frac{1}{c} \frac{\partial I}{\partial t} + \mu \frac{\partial I}{\partial x} + \sigma_t I(x, \mu, t) = \frac{1}{4\pi} \sigma_a a c T^4,$$
$$C_v \frac{\partial T(x, t)}{\partial t} = \sigma_a \phi(x, t) - \sigma_a a c T^4$$

Equations are **nonlinear** and may be tightly coupled

Absorption opacity ( $\sigma_a$ ) can be a strong function of  $T$

# Implicit Monte Carlo (IMC) is the standard Monte Carlo transport method for TRT problems

The system is *linearized* over a time step  $t \in [t^n, t^{n+1}]$   
Opacities are evaluated with  $T(t^n)$

- ▶ Produces a linear transport equation  
with effective emission and scattering terms
- ▶ MC particle histories are simulated  
tallying radiation energy deposition
- ▶ Emission source is **not** fully time-implicit.  
Uses MC integration over  $\Delta t$  for intensity

We developed a **high-order low-order (HOLo)** method that improves on several drawbacks of IMC

## Standard IMC

Large **statistical noise** possible

**Effective scattering** can make MC very expensive

Linearization can cause **non-physical** results (maximum principle violations)

Reconstruction of linear emission shape limits artificial energy propagation

## HOLo Method

ECMC is **very statistically efficient** for TRT problems

MC solution has **no scattering**

Fully **implicit** time-discretization and LO solution **resolves nonlinearities**

Linear-discontinuous FE for  $T(x)$  preserving equilibrium diffusion limit

# A HOLO Algorithm for Thermal Radiative Transfer

---



Overview of algorithm

Derivation of the LO equations

Exponentially Convergent MC High-Order Solver

Computational Results

Extensions and Improvements on HOLO algorithm

# A HOLO Algorithm for Thermal Radiative Transfer



Overview of algorithm

Derivation of the LO equations

Exponentially Convergent MC High-Order Solver

Computational Results

Extensions and Improvements on HOLO algorithm

Basic idea is a nonlinear low-order system with high-order angular correction from Monte Carlo transport solves

The **LO system** is space-angle moment equations, on a fixed finite-element (FE) spatial mesh

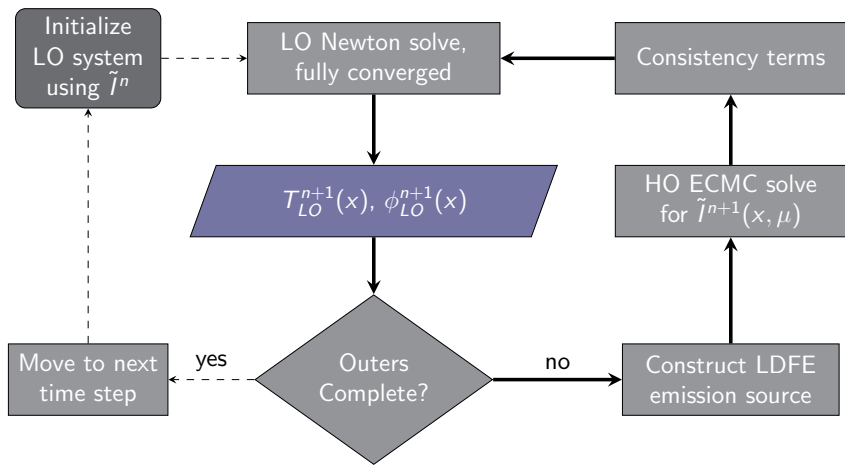
- ▶ Reduced dimensionality in angle  
allows for solution with Newton's method
- ▶ **Output:** linear-discontinuous  $\phi(x)$  and  $T(x)$   
Construct LDFE scattering and emission source

The **HO system** is a pure-absorber transport problem

- ▶ Solved with exponentially-convergent MC (ECMC)  
for *efficient* reduction of statistical noise
- ▶ **Output:** consistency terms



Iterations between the HO and LO systems  
can be performed each time step



# A HOLO Algorithm for Thermal Radiative Transfer

---



Overview of algorithm

Derivation of the LO equations

Exponentially Convergent MC High-Order Solver

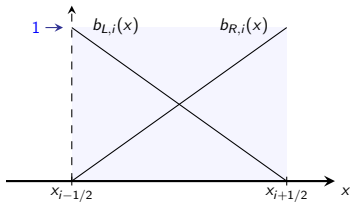
Computational Results

Extensions and Improvements on HOLO algorithm

The LO equations are formed as *consistently* as possible with spatial and angular moments of TRT equations

The time discretization is backward Euler  
for both the HO and LO equations

Spatial moments are weighted with FE basis functions:



$$\langle \cdot \rangle_{L,i} = \frac{2}{h_i} \int_{x_{i-1/2}}^{x_{i+1/2}} b_{L,i}(x)(\cdot) dx$$

Half-range integrals reduce angular dimensionality

$$I^+(x) = 2\pi \int_0^1 I(x, \mu) d\mu$$

Apply moments to the TRT equations  
and manipulate to form **angular consistency terms**

For example, apply  $\langle \cdot \rangle_{L,i}^+$  to a streaming term:

$$\begin{aligned} \left\langle \mu \frac{\partial I}{\partial x} \right\rangle_L^+ &= -\frac{2}{h_i} \{\mu I\}_{i-1/2}^+ + \frac{1}{h_i} [\langle \mu I \rangle_{L,i}^+ + \langle \mu I \rangle_{R,i}^+] \\ &= -\frac{2}{h_i} \frac{\{\mu I\}_{i-1/2}^+}{I_{i-1/2}^+} I_{i-1/2}^+ + \frac{1}{h_i} \frac{\langle \mu I \rangle_{L,i}^+}{\langle I \rangle_{L,i}^+} \langle I \rangle_{L,i}^+ + \frac{1}{h_i} \frac{\langle \mu I \rangle_{R,i}^+}{\langle I \rangle_{R,i}^+} \langle I \rangle_{R,i}^+ \end{aligned}$$

Apply moments to the TRT equations  
and manipulate to form **angular consistency terms**

For example, apply  $\langle \cdot \rangle_{L,i}^+$  to a streaming term:

$$\begin{aligned} \left\langle \mu \frac{\partial I}{\partial x} \right\rangle_L^+ &= -\frac{2}{h_i} \{\mu I\}_{i-1/2}^+ + \frac{1}{h_i} [\langle \mu I \rangle_{L,i}^+ + \langle \mu I \rangle_{R,i}^+] \\ &= -\frac{2}{h_i} \frac{\{\mu I\}_{i-1/2}^+}{I_{i-1/2}^+} I_{i-1/2}^+ + \frac{1}{h_i} \frac{\langle \mu I \rangle_{L,i}^+}{\langle I \rangle_{L,i}^+} \langle I \rangle_{L,i}^+ + \frac{1}{h_i} \frac{\langle \mu I \rangle_{R,i}^+}{\langle I \rangle_{R,i}^+} \langle I \rangle_{R,i}^+ \end{aligned}$$

Now, close the final moment equations:

- Approximate consistency terms with  $\tilde{I}_{HO}^{n+1}$   
from previous HO solve
- Eliminate remaining face unknowns with LD spatial closure  
 $T^4(x)$  and  $T(x)$  also assumed LD

# A HOLO Algorithm for Thermal Radiative Transfer

---



Overview of algorithm

Derivation of the LO equations

Exponentially Convergent MC High-Order Solver

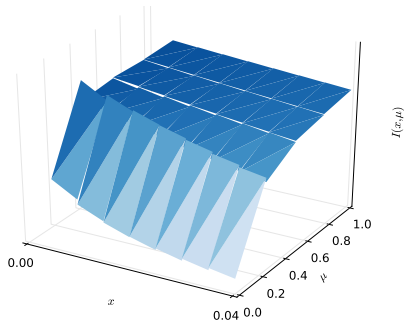
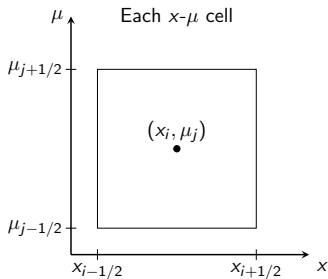
Computational Results

Extensions and Improvements on HOLO algorithm

We use a **projection**  $\tilde{I}(x, \mu)$  onto a space-angle LDFE mesh to represent the solution

local volumetric tallies

$$\tilde{I}_{ij}(x, \mu) = I_a + \frac{2}{h_x} I_x (x - x_i) + \frac{2}{h_\mu} I_\mu (\mu - \mu_i)$$



We apply the ECMC algorithm to the **pure-absorber** HO transport equation

$$\left[ \mu \frac{\partial}{\partial x} + \left( \sigma_t + \frac{1}{c \Delta t} \right) \right] I^{n+1} = \frac{1}{4\pi} \left[ \sigma_a a c (T_{LO}^{n+1})^4 + \sigma_s \phi_{LO}^{n+1} \right] + \frac{\tilde{J}^n}{c \Delta t}$$
$$\mathbf{L} I^{n+1} = q$$

For each batch  $m$ :

- ▶ Evaluate residual source:  $r^{(m)} = q - \mathbf{L} \tilde{J}^{n+1,(m)}$
- ▶ Estimate  $\epsilon^{(m)} = \mathbf{L}^{-1} r^{(m)}$  via **MC simulation**
- ▶ Update solution:  $\tilde{J}^{n+1,(m+1)} = \tilde{J}^{n+1,(m)} + \tilde{\epsilon}^{(m)}$



# I implemented straight-forward variance reduction

## straight-forward variance reduction

$I^n(x, \mu)$  is often an **excellent** estimate of  $I^{n+1}(x, \mu)$   
No MC sampling from thermal equilibrium regions

Histories stream without collision  
along path  $s$ , weight reduces as  $w(s) = w_0 e^{-\sigma_t s}$

Use cell-wise systematic sampling for  $|r^{(m)}|$  source  
Particularly effective in thick cells

- ▶ Particles in each  $x$ - $\mu$  cell  $\propto |r^{(m)}|$  in cell
- ▶ Set minimum  $n$  for cells  
except for cells in thermal equilibrium

# A HOLO Algorithm for Thermal Radiative Transfer

---



Overview of algorithm

Derivation of the LO equations

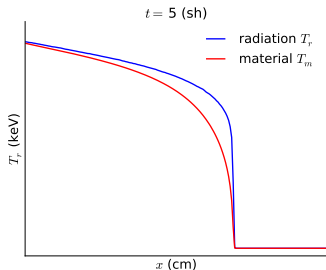
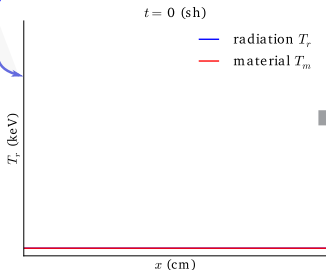
Exponentially Convergent MC High-Order Solver

Computational Results

Extensions and Improvements on HOLO algorithm

We will test our method with several standard **Marshak Wave** problems

constant radiation  
boundary source



Figures depict radiation temperature  $T_r = \sqrt[4]{\phi/ac}$

## Implementation specifics for results are given below:

- ▶ HOLO method implemented as stand-alone C++ code  
IMC results from Jayenne (LANL code)
- ▶  $\Delta t$  increases from 0.01 ns to 0.1 ns
- ▶ One HO solve per time step, with two LO solves
  - ▶ *each HO* solve has 3 ECMC batches  
no adaptive mesh refinement

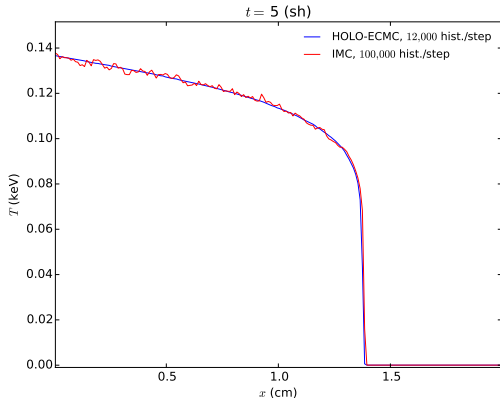
▶ Figure of Merit: 
$$\text{FOM} = \frac{1}{\|\sigma_{\text{rel}}\|^2 N_{\text{total}}}$$

are normalized to IMC results

The HOLO method produces significantly less noise than IMC for a typical Marshak Wave: **FOM=145**

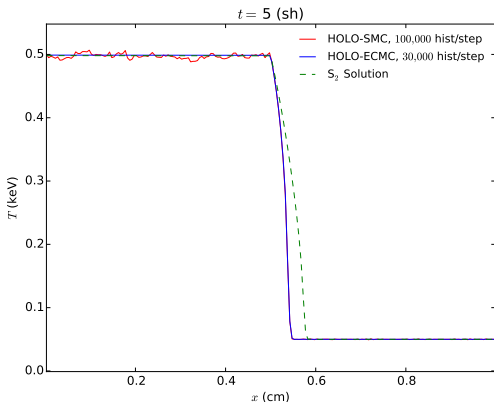
►  $\sigma_a \propto T^{-3}$

- Transient solution after 5 shakes ( $\sim 520$  steps)  
200 x cells (and 4  $\mu$  cells for ECMC)



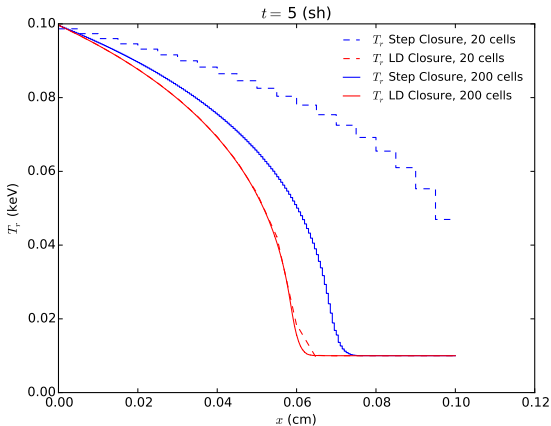
# ECMC is more efficient than standard MC as a HO solver

- ▶ Left half is optically thin ( $\sigma=0.2 \text{ cm}^{-1}$ ), right half is thick ( $\sigma_a=2000 \text{ cm}^{-1}$ ).  $8 \mu$  cells
- ▶ Results for HOLO with different HO solvers:  
ECMC (FOM=10,000), standard MC (FOM=0.46), and an  $S_2$  solution



# The LDFE discretization for the LO equations preserves the equilibrium diffusion limit

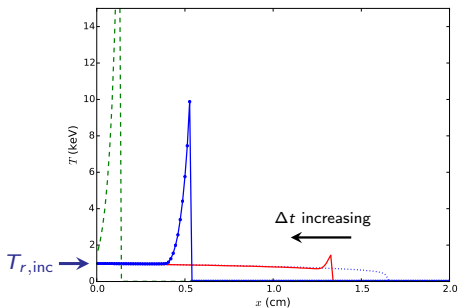
- Large, constant  $\sigma_a$  and small  $c_v$



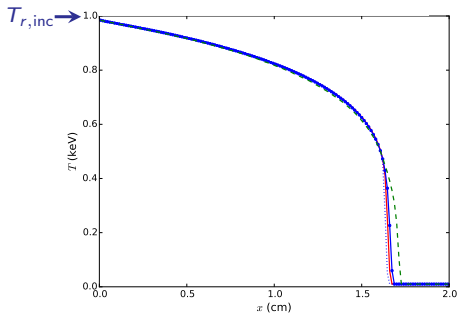
# Our HOLO method preserves the maximum principle with sufficient nonlinear convergence

- ▶ **Material temperatures** plotted; all simulations end at  $t = 0.1$  sh  
 $\sigma_a \propto T^{-3}$ ,  $c_v$  small,  $\Delta t \in [10^{-4}, 10^{-2}]$  sh
- ▶ LO Newton iterations required damping

IMC  $T_m$



HOLO  $T_m$





# A HOLO Algorithm for Thermal Radiative Transfer

---



Overview of algorithm

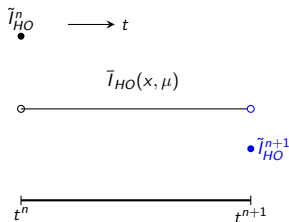
Derivation of the LO equations

Exponentially Convergent MC High-Order Solver

Computational Results

Extensions and Improvements on HOLO algorithm

The time variable can be included in the ECMC trial space with a consistent LO time closure



Include continuous  $\frac{1}{c} \frac{\partial}{\partial t} (\cdot)$  in  $\mathbf{L}$  for residual source leaving  $T(x)$  still implicit

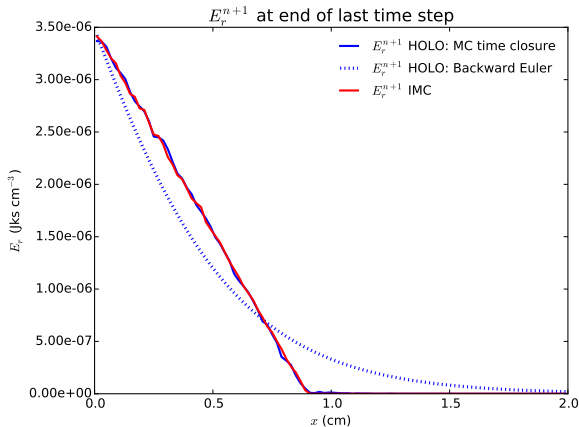
Sample and track particle histories in time.  
Tally the time-averaged and  $t^{n+1}$  error

In **LO equations**, parameterize  $\phi_{LO}^{n+1}$  in terms of **time-averaged** unknowns, e.g.,

$$\langle \phi \rangle_{L,i}^{n+1} = 2 \gamma_{L,i}^{HO} \overline{\langle \phi \rangle}_{L,i} - \langle \phi \rangle_{L,i}^n$$

# The time-closure parameters preserve accuracy of MC time integration in the LO solution

- ▶ Material has  $\sigma_a = 10^{-6} \text{ cm}^{-1}$ , so temperature uncouples  
take 3 large time steps and compare  $E_R^{n+1} = \phi^{n+1}/c$
- ▶ 300,000 histories/step, 100 spatial cells



A few other potential improvements were investigated:

Resolving negative intensities in optically thick cells  
using an artificial source and alternate trial space

Using HO solution to estimate spatial closure  
by including face tallies in ECMC

Source iteration with diffusion synthetic acceleration  
to iteratively solve the LO equations

# A HOLO Algorithm for Thermal Radiative Transfer

---

ECMC is very efficient for TRT simulations  
and fits well in global HOLO context

The LO system can resolve nonlinearities  
with bounded angular consistency terms

Next step is to extend to higher spatial dimensions  
main hurdle to overcome is infrastructure

# A HOLO Algorithm for Thermal Radiative Transfer

---

ECMC is very efficient for TRT simulations  
and fits well in global HOLO context

The LO system can resolve nonlinearities  
with bounded angular consistency terms

Next step is to extend to higher spatial dimensions  
main hurdle to overcome is infrastructure

More details in: S.R. Bolding, M. Cleveland, and J.E. Morel. A HOLO Algorithm with ECMC for Radiative Transfer. NS&E: M&C 2015 Special Issue, 2016. Accepted.

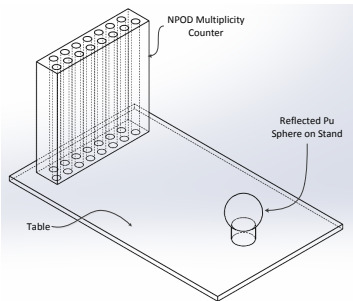
# Simulations of Neutron Multiplicity Experiments with Perturbations to Nuclear Data

Simon Bolding and C.J. Solomon

4 August 2016



# Multiplicity experiments were performed for validating subcritical simulations



\*Not to scale

## Experimental Parameters

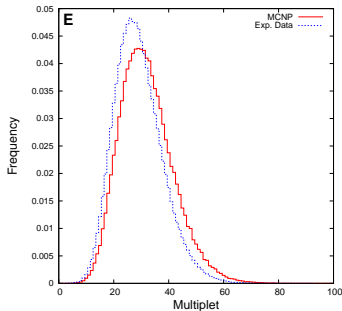
- ▶ 94%  $^{239}\text{Pu}$  sphere
- ▶ 5 reflector configurations  
None to 3.0 cm HDPE shells

Experiments repeated w/  $^{252}\text{Cf}$

C.J. Solomon modeled experiments with modified MCNP5



MCNP5 simulated multiplicity distributions showed discrepancy with experiments for Pu, but not for  $^{252}\text{Cf}$



Pu with 3.0-cm HDPE reflector

Previous work by Mattingly [2010]

- Caused by  $^{239}\text{Pu}$  nuclear data
- Decreased energy-integrated  $\bar{\nu}$ ,  
 $\bar{\nu}$  : mean # of neutrons/fission

**ENDF-VII** raised  $\bar{\nu}$  for  $^{239}\text{Pu}$   
to match  $k_{\text{eff}}$  benchmarks

- $\bar{\nu}$  is  $\sim 2\sigma$  above measured data  
for  $E < 1.5$  MeV

Can we reduce discrepancy in multiplicity distributions without significantly altering  $k_{\text{eff}}$  ?

Perform energy-dependent perturbations of  $\bar{\nu}(E)$  in  $^{239}\text{Pu}$   
Random samples drawn from ENDF-VII.1 covariance data

Compare experimental and simulated multiplicity dist.  
and a  $k_{\text{eff}}$  benchmark (Jezebel)

Compare  $\bar{\nu}(E)$  results to uniform shifts of microscopic cross sections

LANL Python nuclear data library was modified to generate energy-dependent  $\bar{\nu}$  samples

1. Generate a correlated sample of  $\bar{\nu}(E)$ 
  - ▶ Assumed multivariate Gaussian  
with group-averaged covariances
2. Modify continuous  $\bar{\nu}(E)$  data in **ACE** file
3. Perform all MCNP simulations  
with modified ACE data

A cost function provides a measure of inaccuracy for each data realization

Reduced  $\chi^2$  values for the 5 multiplicity experiments and criticality benchmark

$$\chi_{\text{red,mult},m}^2 = \frac{1}{N_{\text{bins}} - 1} \sum_{i=1}^{N_{\text{bins}}} \frac{(P_i^{\text{exp}} - P_i^{\text{mcnp}})^2}{\sigma^2(P_i^{\text{exp}}) + \sigma^2(P_i^{\text{mcnp}})}$$

Equally weight  $\chi^2$  values in a cost function  
A lower score indicates higher accuracy

$$\text{Cost} = \sum_{m=1}^5 \chi_{\text{red,mult},m}^2 + \chi_{\text{red},k_{\text{eff}}}^2$$

Multiplicity and  $k_{\text{eff}}$  simulations were performed for 500 unique realizations of  $\bar{\nu}$  data

Trial	Cost	$\chi^2_{k_{\text{eff}}}$
$\bar{\nu}$ -1.14%	164.24	33.66
<b>303</b>	<b>197.07</b>	<b>4.18</b>
55	267.9	0.01
Original	426.86	0.27

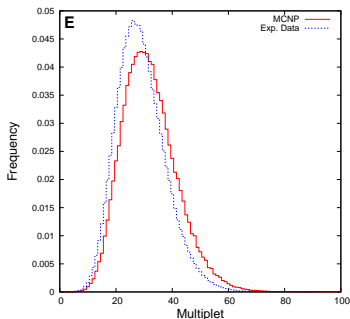
MCNP criticality test suite performed for best data which includes 39 criticality benchmarks w/  $^{239}\text{Pu}$  :

Trial	<i>RMSD</i>
$\bar{\nu}$ -1.14%	1.23%
<b>303</b>	<b>0.51%</b>
Original	0.49%

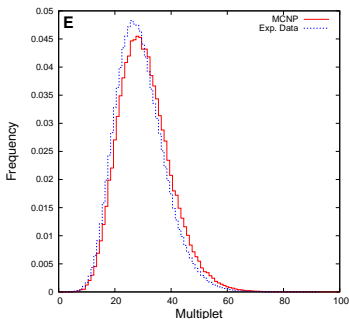
# Energy-dependent $\bar{\nu}$ perturbations improved all 5 multiplicity distributions

- Plots for best data realization and 3.0 cm HDPE case

**Original  $\bar{\nu}$  Data**



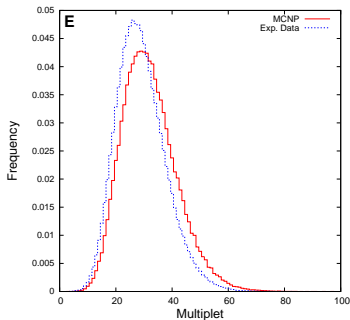
**Trial 303: Lowest Cost**



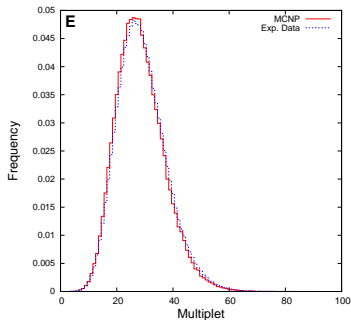
- Best data set reduced **bias** in 1<sup>st</sup> and 2<sup>nd</sup> moments, averaged over all 5 simulations, by  $\sim$  **35%**

Adjusting the fission cross section **uniformly**  
showed good correction to multiplicity simulations

**Original  $\sigma_f$  Data**



**$\sigma_f$  decreased 1.5%**



- High accuracy for all simulations:  $\sum_{i=1}^5 \chi_{red,mult,m}^2 = 14.6$
- $k_{eff}$  is **not preserved**:  $\chi_{k_{eff}}^2 = 22.6$

# Simulations of Multiplicity Experiments with Nuclear Data Perturbations

Energy-dependent  $\bar{\nu}$  perturbations reduced inaccuracies  
in multiplicity while preserving  $k_{\text{eff}}$

- ▶ Majority of cross-correlation terms  $\mathcal{O}(10^{-4})$  or less
- ▶  $\sigma_f$  may need more investigation  
not sensitive to capture cross section

Subcritical simulations should be considered  
in validation of nuclear data

Covariance sampling methodology for nuclear data was  
developed and demonstrated



More details for nuclear data uncertainty work in

S.R. Bolding and C.J. Solomon. Simulations of Multiplicity Distributions with Perturbations to Nuclear Data. Proceedings, ANS Winter Meeting, 2013.

A radiation-hydrodynamics project I did not discuss today was recently submitted to JCP:

S.R. Bolding, J. Hansel, R.B. Lowrie, J.D. Edwards, and J.E. Morel. Second-Order Discretization in Space and Time for Radiation-Hydrodynamics. Journal of Computational Physics, 2016. *Submitted*.

# Simulations of Neutron Multiplicity Experiments with Nuclear Data Perturbations

S.R. Bolding<sup>1</sup>, C.J. Solomon<sup>2</sup>

<sup>1</sup> *Texas A&M University, College station, TX*

<sup>2</sup> *Los Alamos National Laboratory, Los Alamos, NM*

4 August 2016



## Backup Slides

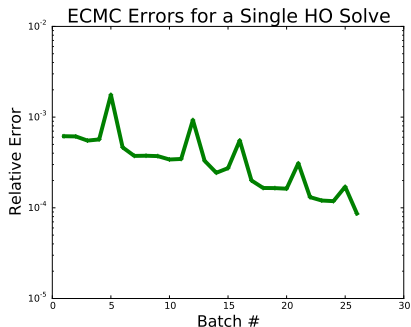
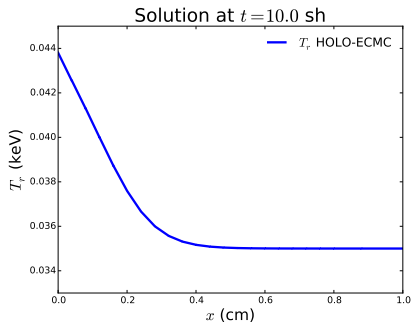
S.R. Bolding<sup>1</sup>, C.J. Solomon<sup>2</sup>

<sup>1</sup> *Texas A&M University, College station, TX*

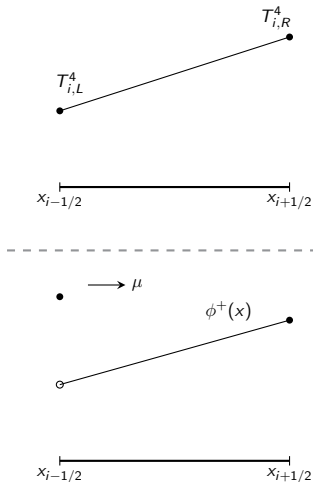
<sup>2</sup> *Los Alamos National Laboratory, Los Alamos, NM*



Exponential convergence can be maintained if the LDFFE mesh resolves the solution reasonably



We can close equations with HO angular information and a linear-discontinuous (LD) spatial discretization



1. Assume  $T(x)$  and  $T^4(x)$  are LD

2. A lagged  $\tilde{I}_{\text{HO}}^{n+1}$  is used to evaluate consistency terms

3. Eliminate  $\phi_{i+1/2}^\pm$  with LD closure preserving equi. diff. limit

$$\phi_{i+1/2}^+ = 2\langle\phi\rangle_{R,i}^+ - \langle\phi\rangle_{L,i}^+$$

4. Global system solved with Newton's method and lagged **implicit opacities**  
Energy is always conserved

We need a way to resolve issues when the LDFF representation of the intensity is negative

Negative intensities can occur in optically thick cells  
Mesh refinement is of minimal use

$\tilde{I}_{HO}(x, \mu)$  must be positive for consistency terms  
to produce a physical, stable LO solution

Independent fix up for LO solution

E.g., lumping or preserving balance with floored  $\phi(x)$

Can add source  $\delta$  to produce a positive projection  $\tilde{l}_{pos}$  such that  $\tilde{l}_{pos}$  satisfies the latest residual equation

Produce  $\tilde{l}_{pos}$  by scaling  $x - \mu$  moments equally,  
to estimate source for the next iteration

$$\begin{array}{ll} \mathbf{L}\tilde{l}^{(m)} = q - r^{(m)} & \longrightarrow \delta^{(m+1)} = \mathbf{L} \left( \tilde{l}^{(m)} - \tilde{l}_{pos}^{(m)} \right) \\ \mathbf{L}\tilde{l}_{pos}^{(m)} = q - r^{(m)} + \delta^{(m+1)} & q \rightarrow q + \delta^{(m+1)} \end{array}$$

We can delay error stagnation

Investigating alternative positive projection of  $l$

# Solving LO System with Newton's Method

- Linearization:

$$\underline{B}(T^{n+1}) = \underline{B}(T^*) + (T^{n+1} - T^*) \left. \frac{\partial \underline{B}}{\partial t} \right|_{t^*}$$

- Modified system

$$[\mathbf{D}(\mu^\pm) - \sigma_a^*(1 - f^*)] \underline{\Phi}^{n+1} = f^* \underline{B}(T^*) + \frac{\underline{\Phi}^n}{c\Delta t}$$

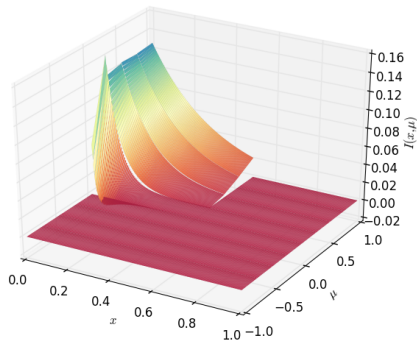
$$\hat{\mathbf{D}} \underline{\Phi}^{n+1} = \underline{Q}$$

$$f = \left( 1 + \sigma_a^* c \Delta t \frac{4aT^{*3}}{\rho c_v} \right)^{-1} \quad T_i^* = \frac{T_{L,i}^* + T_{R,i}^*}{2}$$

- Equation for  $T^{n+1}$  based on linearization that is conservative
- Converge  $T^{n+1}$  and  $\langle \phi \rangle$  with Newton Iterations

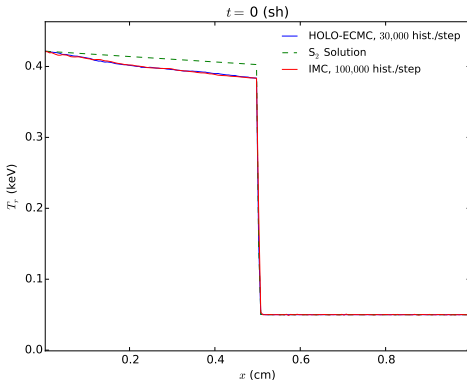


The angular flux for the two material problem is difficult to resolve near  $\mu = 0$



# Two Material Problem, comparison in optically thin region

- Plot of radiation temperature after 10 time steps



Backup slide with timing results

# Forming the LO System

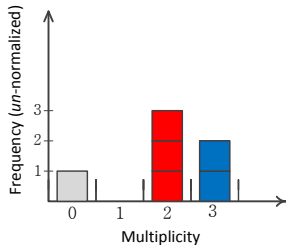
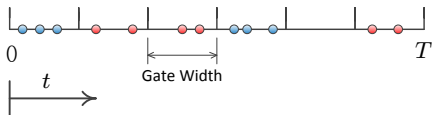
- Taking moments of TE yields 4 equations, per cell  $i$ , e.g.

$$\begin{aligned} & -2\mu_{i-1/2}^{n+1,+} \phi_{i-1/2}^{n+1,+} + \{\mu\}_{L,i}^{n+1,+} \langle \phi \rangle_{L,i}^{n+1,+} + \{\mu\}_{R,i}^{n+1,+} \langle \phi \rangle_{R,i}^{n+1,+} + \\ & \left( \sigma_t^{n+1} + \frac{1}{c\Delta t} \right) h_i \langle \phi \rangle_{L,i}^{n+1,+} - \frac{\sigma_s h_i}{2} \left( \langle \phi \rangle_{L,i}^{n+1,+} + \langle \phi \rangle_{L,i}^{n+1,-} \right) \\ & = \frac{h_i}{2} \langle \sigma_a^{n+1} ac T^{n+1,4} \rangle_{L,i} + \frac{h_i}{c\Delta t} \langle \phi \rangle_{L,i}^{n,+}, \quad (1) \end{aligned}$$

- Cell unknowns:  $\langle \phi \rangle_{L,i}^+$ ,  $\langle \phi \rangle_{R,i}^+$ ,  $\langle \phi \rangle_{L,i}^-$ ,  $\langle \phi \rangle_{R,i}^-$ ,  $T_L$ ,  $T_R$
- Need angular consistency terms and spatial closure (LD)

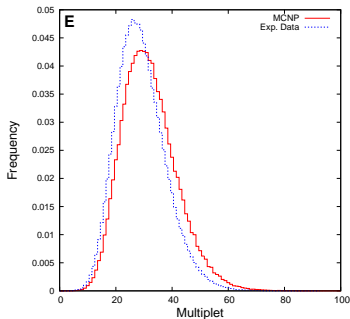
Neutron multiplicity distributions provide passive multiplication information about a fissionable system

○ = Detected Neutron

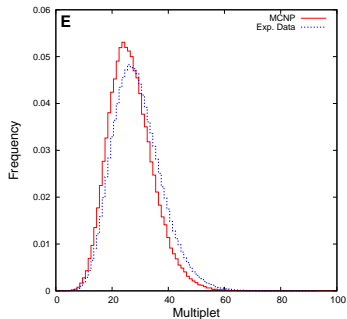


# Energy-Integrated $\bar{\nu}$ Shift – 3.0 cm HDPE reflector

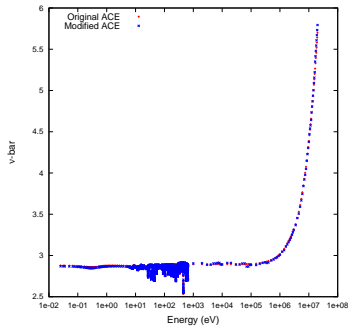
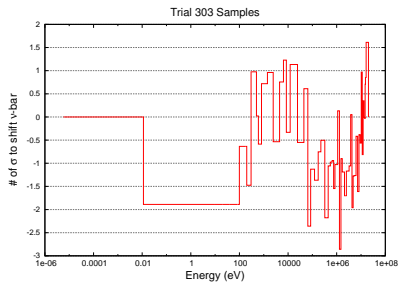
**Original  $\bar{\nu}$  Data**



**-1.14%  $\bar{\nu}$  Data**



# The best $\bar{\nu}$ data (trial 303)



## Fractional shifts to cross sections were made for comparison

Adjusted cross section uniformly at all energies  
compensated with  $\sigma_{tot}$  or  $\sigma_{el}$

Increasing capture cross section was not effective  
relative to variance in data

Scaling fission cross section 1.5% ( $< 1\sigma$ )  
improved multiplicity distributions

- ▶ Adjust elastic scattering ( $\sigma_{el}$ ) to compensate change in  $\sigma_f$ , for  $E > 1$  keV
- ▶ Better improvement than *uniform* scaling of  $\bar{\nu}$